



## Survey geometry influence in PS wave footprint attenuation

Maria Duarte Universidad Eafit\*, William Agudelo, Andrés Calle and Saúl Guevara Instituto Colombiano del Petróleo-ECOPETROL Francisco Gamboa UFBA

Copyright 2011, SBGf - Sociedade Brasileira de Geofísica

This paper was prepared for presentation during the 12<sup>th</sup> International Congress of the Brazilian Geophysical Society held in Rio de Janeiro, Brazil, August 15-18, 2011.

Contents of this paper were reviewed by the Technical Committee of the 12<sup>th</sup> International Congress of the Brazilian Geophysical Society and do not necessarily represent any position of the SBGf, its officers or members. Electronic reproduction or storage of any part of this paper for commercial purposes without the written consent of the Brazilian Geophysical Society is prohibited.

### Summary

We defined the acquisition footprint as any pattern of noise that is highly correlated to the geometric distributions of sources and receivers on the earth's surface. Footprint is especially annoying in PS data acquisition, in contrast to PP in which the attenuation techniques works properly in processing stages. Generally footprint is attenuated during the processing stages but the best strategy is to avoid it since the beginning in order to preserve the signal character.

This paper focuses in analyzing the influence of acquisition geometries on footprint. We test three PS acquisition geometries with the same design parameters, except the receiver and/or source spatial distribution. In order to determine, qualitatively and quantitatively, the geometry that provides the smaller amplitude, offsets vs azimuth and wave number charts are analysed.

### Introduction

In recent years, there have been a rising interest in converted-wave surveys, however the theory of multicomponent survey design is not well established. Only few studies have centered its attention on integrate imaging and footprint attenuation, Cary (2007a) have examined the efficacy of orthogonal versus slant survey design for 3D PS surveys, and proposed a sparse shot approach to improve offsets and azimuth uniqueness within common-conversion point (CCP) gathers. Cordsen (2004) proposed a way to smooth fold distributions introducing an element of randomization into the geometry of the field layout. Vermeer (1990) suggests that 3-D arrays should be used on both sources and receivers to properly suppress steep-dip, high-energy, side scattered noise.

### Theory

The footprint is the time variant and spatial variant pattern of amplitude distortion in the 3D/3C seismic volume due solely to the 3D geometry. Each stacking bin contains a slightly different fold and a different mix of offsets that get stacked to the final PSTM migrated trace (Cordsen, et al

2000). This spatially varying amplitude distortion is due to two effects: First, different effective fold values in different bins result in different post-stack S/N ratios operating on the random noise in the CMP or CCP gathers. Secondly, the residual organized noise, either residual lineal noise or residual multiple reflection have different expressions at different offsets. Hence a different mix of offsets in different bins stacks a different combination of residual organized noise. The combined effect of these two processes is to create a regular spatial and temporal pattern of amplitude distortion in the 3D/3C volume which is superimposed on amplitude variations due solely to geology (e.g. reflectivity, porosity, fluids etc).

There are three main techniques used to reduce the generation of acquisition footprints (Zhang, 2009):

- (1) Acquisition geometries which produce a minimal variation of the bin-to-bin population of trace offsets.
- (2) Via prestack process which minimize the offsets-related amplitude differences among traces prior to stacking.
- (3) Using poststack processes, such as f-k, and Kx-Ky filtering.

### Methodology and case study

The methodology consists in two steps. The first created three geometries in reference basic parameters. The second consists took crossline with object quantify with geometry have less amplitude oscillation.

(I) Tenerife 3D3C field design preplot parameters (Table 1) were used and the shot and receptor positions were displaced with the aim to create three seismic acquisition geometries

Acquisition parameters for the Tenerife 3D3C survey	
Receiver interval	20m
Shot interval	20m
Bin size	10x10
Shot line interval	360
Receiver line interval	280
Channel number	3456 x3 multicomponent
Nominal fold	48
Aspect radio	0.964
Fold in-line	6
Fold Crosline	8
Relación Vp/Vs	1.78
Target depth	2200 m
Target time	1800

**Table 1.** Parameters for the Tenerife 3D3C survey (Ecopetrol, 2009).

The designed geometries are the following (Figure 2):

**(a) Orthogonal:** It is identical to preplot geometry of Tenerife field and was used as comparison base.

**(b) Random:** The shots were randomly moved preserving the distance between shot lines. The maximum displacement contemplated was 20 meters which is equal to the distance between shot points. Nevertheless, Duarte (2010) determined that displacements from 5 to 7 meters attenuate better the footprint.

**(c) Slant:** The angle between receiver lines and shot lines was setup to 26.5 degrees

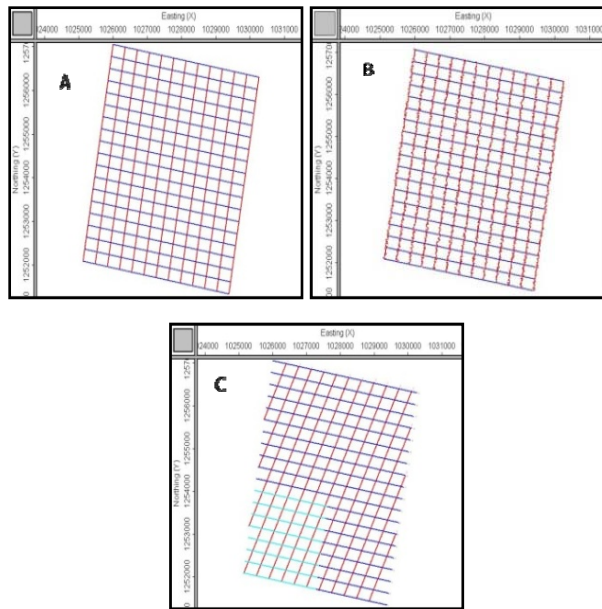


**Figure 2.** Acquisition Geometry a) Orthogonal, b) Randomize, c) Slant.

We generated the following quality diagrams for three proposed geometries: fold, offsets and azimuth distribution and Fourier analysis with the goal of determine which geometry improves the footprint attenuation.

**(a) Fold diagram**

Shows, using a color scale, the spatial distributions of the number of reflection points or mode conversion points that fall into a single bin. The stacking bin size must contain enough fold to allow for the required post-stack PP and PS S/N ratios.

The figure 3 shows the comparison of nominal PS fold for the three candidate 3D3C design geometries for a typical box in the full fold area. These fold values are computed for the natural bin size (RI/2) for each survey.

The footprint is better attenuated in slant geometries than in the orthogonal and random ones (Figure 3).

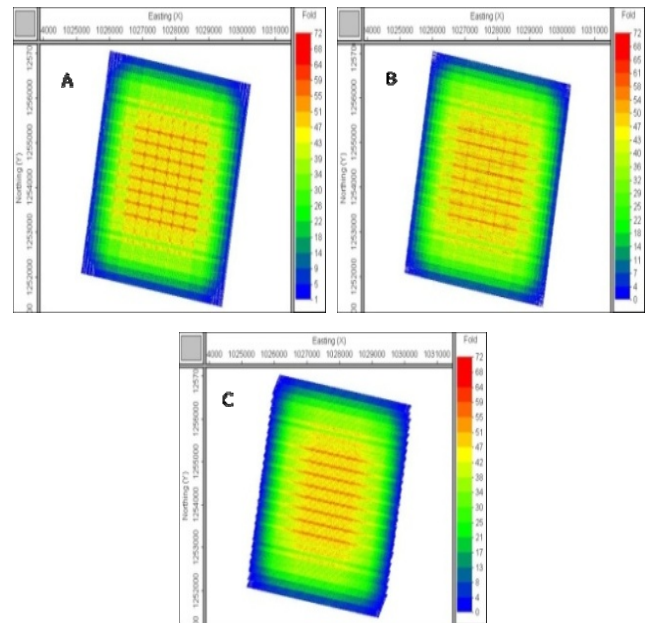


**Figure 3.** Fold PS. A) Orthogona. B) Randomize C) Slant

**(b) Offsets diagram:**

In this diagram, the horizontal and vertical axes are bin number and offsets. For the Inline version of this chart (Figure 4), the bins within the box are sampled in the inline direction snaking through the subset area in the xline direction. Withing each bin, voxel for each offset present in the bin color coded according to the offsets fold redundancy. If a given unique offset is absent in a bin, the voxel corresponding to that unique offsets is left blank or white. If the offset are represent, the voxel is color coded according to the number of time that offset occurs in the bin. As with the stick chart display, efficiently acquired 3D3C surveys will show mostly blue offsets fold redundancies (acquiring a given unique offsets only once per bin) and will show fewer and smaller holes of white (missing offsets) in the offsets distributions. These bin offsets fold redundancy charts are good for seeing how well unique offsets are sampled and distributed within adjacent bins. The chevron pattern of the near offsets is function of the effect of Xmin in an orthogonal survey.

In Figure 4 it is possible to see the effective PS fold for the all candidate 3D/3C design geometries for a typical box in the full fold area, with offsets limited to the usable PS offsets range of 300 to 2,950m. This fold is made for final stacking bins equal in size to the RI and SI for each design.

Figures 4.a-b-c contains the same footprint pattern, but the random geometry shows smooth that these pattern.

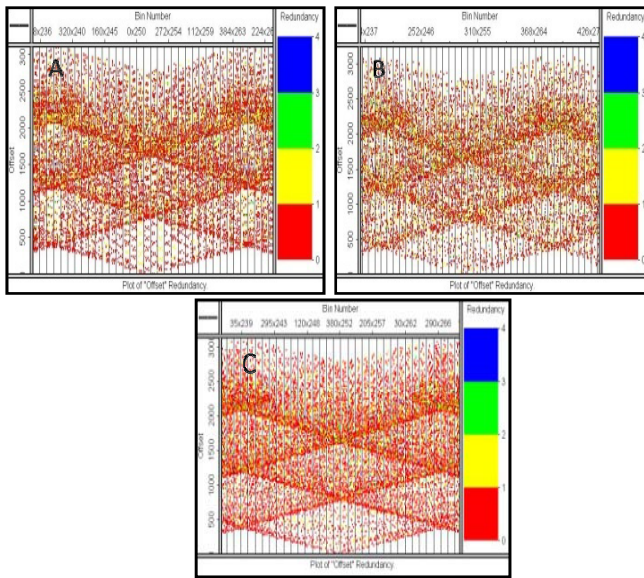


**Figure 4.** Offsets Fold PS redundancy. A) Orthogonal. B) Randomize C) Slant.

**(c) Azimuth diagram:**

In this diagram, the horizontal axis is a bin number and vertical axis is azimuth. For the Inline version of this chart (Figure 5), the bins within the box are sampled in the inline direction snaking through the subset area in the xline direction. Withing each bin, voxel for each azimuth present in the bin color coded according to the azimuth fold redundancy.

Figure 5 shows that the orthogonal, random and slant geometries have gaps around 100 degrees of azimuth.

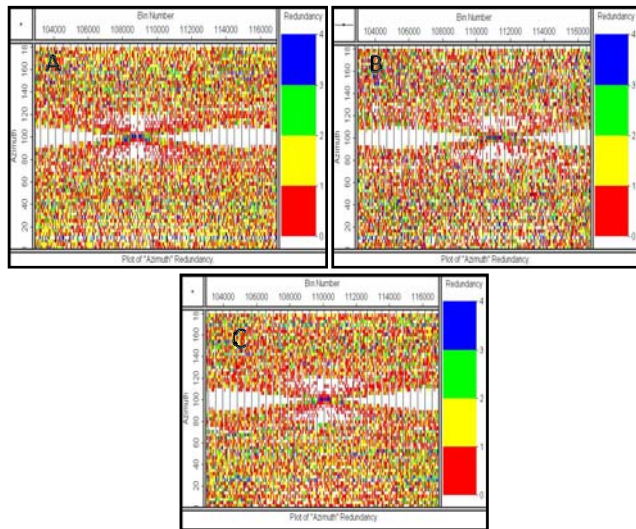


**Figure 5.** Offsets Fold PS redundancy. A) Orthogonal. B) Randomize C) Slant.

**(e) Fourier analysis:**

It is important to minimize the strong variations in the wave number in order to avoid the signal aliasing.

The figure 6 show the inline PS stack section through the center of the 3D footprint analysis stack cube generated for each candidate 3D3C. The seismic stack amplitudes are color coded blue (minimum) and red (maximum). And again, a minimal footprint response will have a small range in amplitudes along a given horizon.

In Figure 6 appears the distribution of the amplitude in the design area as a function of the inline and crossline wave number. Figure 6B and 6C show that the amplitude variation is spatially smaller than compared with the orthogonal.

In Figure 6.C is evident the shot footprint along the diagonal direction while this is not visible in the fold chart (Figure 3.A)

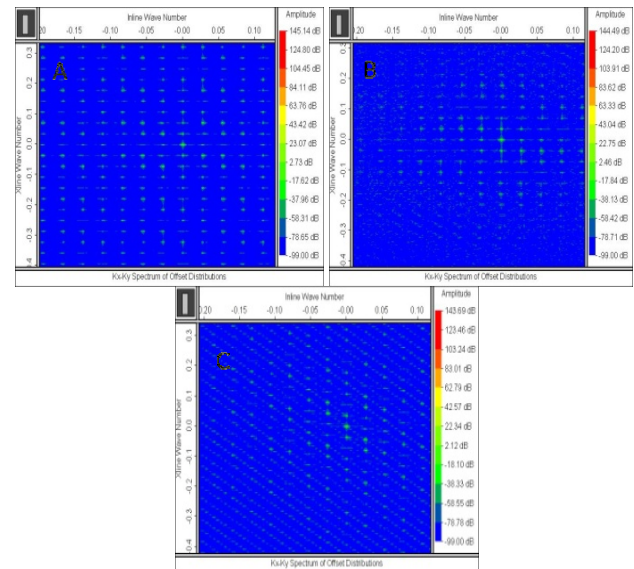


**Figure 6.** Fourier analysis. A) Orthogona. B) Randomize D) Slant.

(II) In this step we analyzed how fold change for inline 6-7 in each geometry: orthogonal, random, and slant (Figure 7).

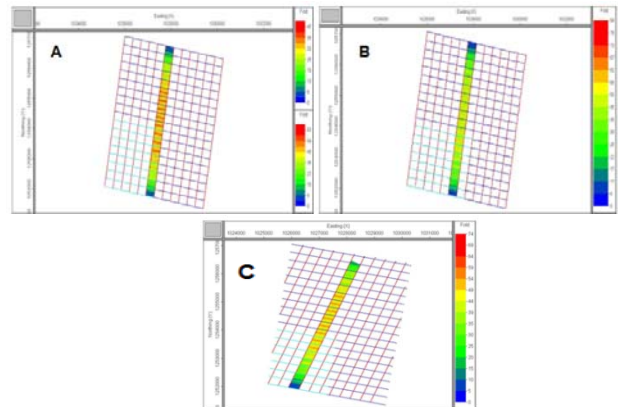


**Figure 7.** Fold PS diagram for segment crossline 6-7 A). Orthogonal, B). Random, C). Slant (Duarte, 2010).

In this step, Sps information for each geometry (Orthogonal, random, diagonal) from 6 and 7 crosslines (Figure 7) were used in order quantify the fold variations and identify the number of oscillation patterns for each geometry (Orthogonal, random, diagonal) (Figure 8).

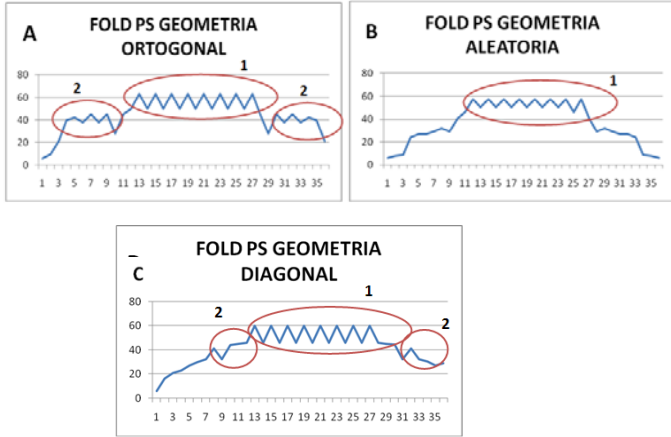


**Figure 8.** Fold distribution for the *crosslines* 6 and 7. A) Orthogonal geometry, b). Random geometry. c) diagonal geometry (Duarte, 2010).

Orthogonal and Slant geometry have the highest pattern number. For the orthogonal geometry it varies between 50-63 and 45-38. On the other hand the Slant geometry presents patterns numbers varying between 46-60 and 41-32 (Table 1). Table 1 summarizes the results:

Geometry	Pattern 1 (Fold)	Variance for Pattern 1	Pattern 2 (Fold)	Variance for Pattern 2
Ortogonal	50-63	13	45-38	7
Random	46.7-50.5	3.8	-----	-----
Diagonal	46-60	14	41-32	9

**Table 1** Fold oscillation pattern of receiver lines for three different geometries.

Geometry with smaller number pattern values is diagonal (Figure 8.C). But the geometry with the small variance value in the oscillation pattern was the random geometry (Table 1).

**Conclusions**

According to the fold diagram, the diagonal geometry attenuates footprint on shot lines (Lawton, 2003). However an analysis of this geometry in the wavenumber domain allows identify the footprint in the diagonal direction of shot lines.

Highest randomness does not guaranty to get footprint decreased. For this reason is very important to do a preliminary study in which the optimum percentage of randomness for footprint attenuation can be determined.

In general, random geometry presents less oscillation in fold values due to footprint in receiver lines. The footprint effect is more evident when orthogonal and diagonal geometries are used.

**Acknowledgments**

The authors would like to thank the Colombian Petroleum Institute of ECOPETROL for their cooperation in providing the data, support and for permission to publish this work.

**References**

Cary, P., 2007a, 2-D Migration Footprint: CSEG Recorderm 32m no 6, 22-24.

Cordson A., 2004. Acquisition Footprint Can Confuse. AAPG Explorer, March 2004.

Cordson, A Galbraith, M., and Peirce, J., 2000., Planning land 3-D surveys, Geophysical developments No 9, Hardage, B.A., ed., Society of Explorations Geophysicists.

Duarte, M., 2010. Análisis de Sensibilidad en el diseño de parámetros de adquisición sísmica 3D3C para el Campo Tenerife. Tesis de Maestría, Universidad Eafit.

Ecopetrol, 2009, Tenerife 3D/3C Seismic Evaluation and Design, v1 p5.

Lawton, D.C., 2003, Considerations in 3-D depth-specific P-S survey design. CREWES Project, Annual Research Report, Volume 15.

Vermeer, G. J. O., 1990, Seismic wavefield sampling: A wavenumber approach to acquisition fundamentals, in Cooper, M. R., Ed., Geophysical references 4: Soc. Expl. Geophys.

Rui Zhang., 2009. Footprint suppression with basis pursuit denoising. SEG Houston International Exposition and Annual Meeting.